

Two distinct transitions in a population of coupled oscillators with turnover: desynchronization and stochastic oscillation quenching

Ayumi Ozawa* and Hiroshi Kori

Graduate School of Frontier Sciences, The University of Tokyo, Chiba 277-8561, Japan

(Dated: July 7, 2023)

Synchronization due to mutual coupling and turnover, or the replacement of old components with new ones, are ubiquitously observed in open systems consisting of many components. Although these phenomena can co-occur, the synergistic effects of coupling and turnover have been overlooked. Here, we analyze coupled phase oscillators with turnover and reveal that two distinct transitions occur, depending on both coupling and turnover: desynchronization and what we name stochastic oscillation quenching. Importantly, the latter requires that both the turnover and coupling are sufficiently intense.

Introduction The emergence of order in an open system composed of many interacting units is widely observed in nature. Particularly, mutual synchronization is observed in a wide range of coupled oscillator systems[1], from biological ones[2, 3] to social[4, 5] and artificial ones[6, 7]. Another phenomenon broadly found in open many-body systems is turnover due to the addition and removal of the components. Examples include the protein and cell turnover in biological systems[8, 9]. Other examples are found in social[10, 11] and bio-inspired chemical systems[12]. Also, a growing population may be effectively modeled as a system with turnover if the growth causes the dilution of the components[13, 14]. These two phenomena, mutual synchronization and turnover, may realize in the same system, and their time scales are not always clearly separated. For example, KaiC proteins in a cyanobacterial cell show the collective rhythm of phosphorylation and dephosphorylation with a period of about 24h, and their average half-life is estimated to be about 10h[15].

Recent studies have revealed that turnover can deteriorate collective oscillation; it has been shown numerically[13] and experimentally[16] that the synchronized phosphorylation-dephosphorylation cycles of KaiC proteins become less robust when the turnover rate is a sufficiently large constant. Moreover, Ref. [13] has suggested that their collective oscillation disappears when the turnover rate is further increased. However, little attention has been paid to the synergistic effect of the turnover with the interaction among oscillators, which is essential for mutual synchronization. In particular, these previous studies lack analyses on how the effect of the turnover changes as the properties of the coupling are varied.

Here, we study a simple model of coupled phase oscillators with turnover and show that their collective oscillation disappears via two distinct transitions depending on both the coupling and turnover; for sufficiently small coupling strengths, the collective oscillation is lost via desynchronization[17] as the turnover rate is increased, while for stronger coupling strengths, we may observe what we name *stochastic oscillation quenching* (SOQ), which can be interpreted as a stochastic analog of oscillation quenching[18]. Interestingly, the analysis indicates that SOQ may be induced not only by increasing the turnover rate but also by strengthening the interaction among oscillators; thus this extinction of the collective oscillation is caused by a synergistic effect of the turnover and coupling. Our model is based on the Kuramoto model[17, 19–21], which has been successfully applied to investigate synchronization in various systems[1, 3, 5, 7, 22, 23], and incorporates the effect of the turnover as stochastic resetting[24]. The tractability of the model enables us to obtain transition curves.

The Kuramoto model with turnover The dynamics of N identical Kuramoto oscillators are given as follows[17, 19]:

$$\frac{d\theta_i}{dt} = \omega + \frac{\kappa}{N} \sum_{j=1}^N \sin(\theta_j - \theta_i), \quad (1)$$

where θ_i ($i = 1, 2, \dots, N$) is the phase of the i th oscillator, $\omega \neq 0$ is the natural frequency of the oscillators, and $\kappa \geq 0$ represents the coupling strength.

Suppose one of the oscillators is randomly chosen and replaced with a new oscillator. This event is equivalent to resetting the phase of the chosen oscillator to that of the newly added one. Hence, as a model of oscillators with turnover, we adopt a system that involves phase resetting. Specifically, we consider a population of Kuramoto oscillators where each oscillator experiences the reset event with probability αdt during an infinitely short time width dt so that αN oscillators are expected to be substituted per unit time. Such dynamics can be described by the

following Itô stochastic differential equation with jumps:

$$d\theta_i = \left[\omega + \frac{\kappa}{N} \sum_{j=1}^N \sin(\theta_j - \theta_i) \right] dt + [-\theta_i + \phi(\gamma_i)] dP_i(\gamma_i; \alpha) \quad (2)$$

where the last term describes the stochastic reset of θ_i to a new phase ϕ that is drawn from a distribution $f(\phi)$ at each reset. More precisely, this term is the differential of a Poisson process with state-dependent and mark-dependent amplitudes[25], where γ_i is the underlying mark variable and α is the constant jump rate. Hereafter we call α turnover rate. The counting processes $\{P_i(\gamma_i; \alpha)\}_{i=1}^N$ are pairwise independent. In other words, the timings of the resets of two different oscillators are independent. The distributions of the mark variables are set to be uniform in $[0, 2\pi)$, and the function $\phi(\gamma)$ is determined so that the distribution of ϕ is given by $f(\phi)$.

Consistent with the previous work[13], the increase of the turnover rate α in Eq. (2) causes the extinction of the macroscopic oscillation. The snapshots of the phase distribution in FIG. 1(a,b) indicate that the distribution for $\alpha = 0.1$ has a sharp peak and changes with time, while that for $\alpha = 0.3$ is almost uniform and steady. In the numerical simulation, we adopted $f(\phi)$ that has the form of the Poisson kernel:

$$f(\phi) = \frac{1}{2\pi} \frac{1 - \sigma^2}{1 - 2\sigma \cos \phi + \sigma^2}, \quad (3)$$

where σ determines the sharpness of $f(\phi)$; $f(\theta) = 1/(2\pi)$ for $\sigma = 0$ and $f(\theta) \rightarrow \delta(\theta)$ as $\sigma \rightarrow 1$. Other unimodal distributions yielded similar results (not shown here).

Let us quantify the macroscopic oscillation by introducing the complex order parameter r , Kuramoto order parameter R , and mean phase Θ as follows[17, 20]:

$$r(t) = R(t)e^{i\Theta(t)} := \frac{1}{N} \sum_{j=1}^N e^{i\theta_j(t)}. \quad (4)$$

With this definition, R reflects the coherence of the phases; $R = 0$ when the phases are uniformly distributed, and $R = 1$ when all oscillators have the same phase. Note that the system without the turnover, Eq. (1), has a stable synchronized oscillatory solution with $R(t) = 1$ and $\Theta(t) = \Theta(0) + \omega t$. The time series of $\text{Re}(r)$ oscillates for $\alpha = 0.1$, while it is constant for $\alpha = 0.3$; see Fig. 1(c).

We define the intensity of the macroscopic oscillation to be the fluctuation of r :

$$Q := \sqrt{\langle (r - \langle r \rangle_t)^2 \rangle_t}, \quad (5)$$

where $\langle \cdot \rangle_t$ denotes the long-time average. Note that $Q = 0$ if r is constant. As shown in Fig. 2, the dependency of Q on phase resetting qualitatively changes as the coupling strength κ varies. For sufficiently small κ , the value of Q is hardly affected by the width σ of the distribution f and gradually decreases as α increases. In contrast, for larger values of κ , σ also affects Q ; when $\sigma \simeq 0$, Q gradually decreases as α increases (Fig. 2(a)) while Q suddenly drops to near 0 when $\sigma \simeq 1$ (Fig. 2(b)).

Mean-field approximation To analyze these transitions, let us reduce the system by employing the mean-field approximation in the same spirit as [26]. Firstly, let $p(\boldsymbol{\theta}, t)$ and $p_i(\theta_i, t)$ be the probability density function for $\boldsymbol{\theta} := (\theta_1, \theta_2, \dots, \theta_N)$ at time t and its marginalization over all phase variables except θ_i , respectively. From Eq. (2), the time evolution of $p_i(\theta_i, t)$ is given as follows[25]:

$$\frac{\partial p_i}{\partial t} = -\frac{\partial}{\partial \theta_i} \left[\int_{S_i} p(\boldsymbol{\theta}, t) v_i(\boldsymbol{\theta}, t) d\boldsymbol{\theta}_i \right] + \alpha f - \alpha p_i, \quad (6)$$

where $\boldsymbol{\theta}_i := (\theta_1, \theta_2, \dots, \theta_{i-1}, \theta_{i+1}, \dots, \theta_N)$, $\int_{S_i} \cdot d\boldsymbol{\theta}_i := \int_0^{2\pi} \dots \int_0^{2\pi} \cdot d\theta_1 d\theta_2 \dots d\theta_{i-1} d\theta_{i+1} \dots d\theta_N$, and $v_i(\boldsymbol{\theta}, t) := \omega + \kappa N^{-1} \sum_{j=1}^N \sin(\theta_j - \theta_i)$.

Now we invoke the mean-field approximation; we assume $p_i(\theta_i, t)p_j(\theta_j, t) - p_{i,j}(\theta_i, \theta_j, t) \rightarrow 0$ and $p_i(\theta_i, t) - p_j(\theta_j, t) \rightarrow 0$ as $N \rightarrow \infty$ for any $i \neq j$, where $p_{i,j}(\theta_i, \theta_j, t)$ is the joint probability distribution function for θ_i and θ_j . Then,

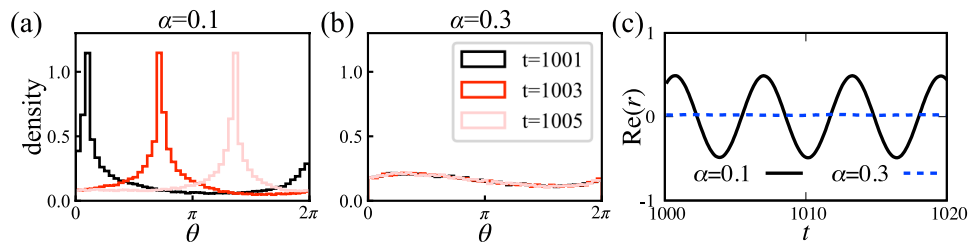


FIG. 1: An increase in the turnover rate α quenches the collective oscillation. (a), (b) Snapshots of the phase distribution for $t = 1001$ (black), $t = 1003$ (red), and $t = 1005$ (light pink), obtained from the numerical simulation of Eq. (2) by Euler-Maghsoudi method[25]. (a) The propagation of the distinct peak of the distribution is observed for $\alpha = 0.1$. (b) For $\alpha = 0.3$, the distribution is steady and also flatter compared to $\alpha = 0.1$. (c) Time series of the real part of the complex order parameter r . The black solid and blue dotted curves show the dynamics of $\text{Re}(r)$ for $\alpha = 0.1$ and $\alpha = 0.3$, respectively. The oscillation observed for $\alpha = 0.1$ disappears for $\alpha = 0.3$. In all the simulations, the initial state is the uniform distribution. Other parameters are $\kappa = 0.3$, $\sigma = 0.5$, and $N = 50000$.

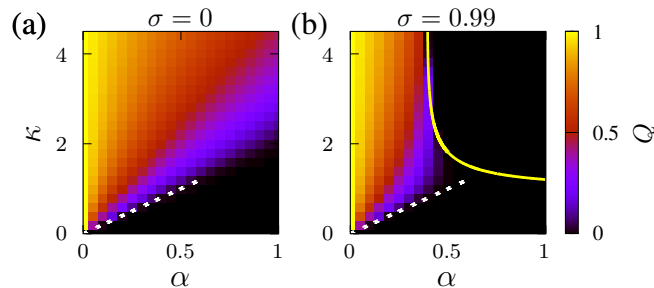


FIG. 2: Two transition curves explain the disappearance of the collective oscillation. The index Q of the intensity of the collective oscillation, defined by Eq. (5), is averaged over 5 realizations of the Poisson processes and shown in color scale for (a) $\sigma = 0$ and (b) $\sigma = 0.99$. When α and κ are sufficiently small, the critical coupling strengths below which Q vanishes coincides with the desynchronization transition curve, $\kappa = \kappa_c$, which is shown with white dotted line in both panels. In contrast, when κ is sufficiently large, the boundary of collective oscillation depends on σ ; in (a), the boundary depends on κ almost linearly even for $\alpha \sim 1$, while in (b), another transition curve in addition to $\kappa = 2\alpha$ is needed to fully describe the boundary. The supplementary curve obtained by analyzing SOQ is shown by yellow solid curve. The initial condition is set to the uniform distribution, and the number of oscillators is $N = 2000$.

Eq. (6) yields the time evolution equation of the phase distribution $p(\theta, t)$ as follows:

$$\frac{\partial p}{\partial t} = -\frac{\partial}{\partial \theta} [pv] + \alpha f - \alpha p, \quad (7)$$

$$v = v(\theta, t) := \omega + \kappa \int_0^{2\pi} p(\tilde{\theta}, t) \sin(\tilde{\theta} - \theta) d\tilde{\theta}. \quad (8)$$

Hereafter we set $\omega = 1$ without the loss of generality by normalizing t , ω , and α by ω .

Desynchronization When $\alpha = 0$, Eq. (7) has the uniform steady solution $p^{(0)}(\theta) := 1/(2\pi)$. This solution corresponds to the desynchronized state in the sense that the cohesiveness of the phases is completely lost. For $\alpha \neq 0$, $p^{(0)}(\theta)$ is no longer a solution of Eq. (7), but FIG. 1(b) suggests the existence of a steady solution that is obtained by slightly deforming $p^{(0)}(\theta)$. The stabilization of such a solution, formally analyzed below, explains the extinction of the collective oscillation observed for small κ and α in Fig. 2.

Let ρ be the deviation from a steady solution \hat{p} , i.e., $\rho = p - \hat{p}$. By linearizing Eq. (7) around \hat{p} , we obtain

$$\frac{\partial \rho}{\partial t} \simeq -\frac{\partial}{\partial \theta} \{ \hat{p} \mathcal{U}[\rho] + (1 + \mathcal{U}[\hat{p}]) \rho \} - \alpha \rho =: \mathcal{L}[\rho], \quad (9)$$

where the linear functional \mathcal{U} is defined by

$$\mathcal{U}[\rho](\theta) := \kappa \int_0^{2\pi} \sin(\tilde{\theta} - \theta) \rho(\tilde{\theta}) d\tilde{\theta}. \quad (10)$$

In addition, let us assume that \hat{p} and \mathcal{L} are expanded as follows for sufficiently small values of α :

$$\hat{p}(\theta; \alpha, \kappa) = \hat{p}^{(0)}(\theta) + \sum_{l=1}^{\infty} \alpha^l p^{(l)}(\theta; \kappa), \quad (11)$$

$$\mathcal{L} = \sum_{l=0}^{\infty} \alpha^l \mathcal{L}^{(l)}. \quad (12)$$

The expression for $\mathcal{L}^{(l)}$ is obtained by inserting Eqs. (11) and (12) into Eq. (9) and collecting the terms of $\mathcal{O}(\alpha^l)$. It is straightforward to find that $\mathcal{L}^{(0)} u_m^{(0)}(\theta) = \lambda_m^{(0)} u_m^{(0)}(\theta)$ holds for any integer m , where $u_m^{(0)}(\theta) = e^{im\theta}$ and $\lambda_m^{(0)} = -im + \frac{\kappa}{2} \delta_{|m|,1}$.

Now we define an inner product $\langle \cdot, \cdot \rangle$ of smooth 2π periodic functions $z_1(\theta)$ and $z_2(\theta)$ by

$$\langle z_1, z_2 \rangle := \frac{1}{2\pi} \int_0^{2\pi} z_1(\theta) \overline{z_2(\theta)} d\theta, \quad (13)$$

where $\overline{z_2(\theta)}$ is the complex conjugate of $z_2(\theta)$. The adjoint operator $\mathcal{L}^{(0)*}$ of $\mathcal{L}^{(0)}$ defined on this inner-product space satisfies $\mathcal{L}^{(0)*} u_m^{(0)} = \lambda_{-m}^{(0)} u_m^{(0)}$. Thus, $u_m^{(0)}(\theta)$ is an eigenvector of both $\mathcal{L}^{(0)}$ and $\mathcal{L}^{(0)*}$. This allows us to apply Rayleigh-Schrödinger perturbation theory[27] to evaluate the eigenvalues of \mathcal{L} . Specifically, we assume that the eigenvalues and eigenvectors of \mathcal{L} can be expanded around that of $\mathcal{L}^{(0)}$:

$$\mathcal{L} u_m = \lambda_m u_m, \quad (14a)$$

$$u_m = \sum_{l=0}^{\infty} \alpha^l u_m^{(l)}, \quad \lambda_m = \sum_{l=0}^{\infty} \alpha^l \lambda_m^{(l)}. \quad (14b)$$

To ensure the uniqueness of the expansion, we also impose the orthogonality condition $\langle u_m^{(0)}, u_l^{(0)} \rangle = \delta_{0,l}$.

Inserting Eqs. (12) and (14b) into (14a) and extracting the terms of $\mathcal{O}(\alpha)$, we obtain

$$\lambda_m^{(1)} u_m^{(0)} = \mathcal{L}^{(0)} u_m^{(1)} + \mathcal{L}^{(1)} u_m^{(0)} - \lambda_m^{(0)} u_m^{(1)}. \quad (15)$$

Then, computing the inner product $\langle \lambda_m^{(1)} u_m^{(0)}, u_m^{(0)} \rangle$ yields $\lambda_m^{(1)} = -1$. Hence $\lambda_m = -im + \delta_{|m|,1} \frac{\kappa}{2} - \alpha$ to the order of α , and the maximum of the real parts of the eigenvalues exceeds 0 when

$$\kappa \simeq 2\alpha =: \kappa_c. \quad (16)$$

Figure 2 implies that, for small α , the boundary on which Q vanishes agrees with the curve $\kappa = \kappa_c$, which is shown with the white dotted curves. Consistent with the numerical simulation, κ_c depends on α but not on σ , the width of $f(\theta)$.

It should be noted that the stability analysis here is formal but not mathematically rigorous because (1) the validity of the perturbative calculation is assumed without any proof and (2) the continuous and residual spectra are ignored. Nevertheless, the agreement with numerical simulation indicates the validation of the analysis.

Stochastic oscillation quenching The dependency of Q on the turnover rate α for $\sigma = 0$, shown in Fig. 2(a), does not qualitatively change when κ is increased. However, when σ approaches 1, the transition observed for large κ is no longer explained by desynchronization discussed above; see Fig. 2(b).

Numerical simulation indicates that the phase distribution after this transition is steady but far from uniform, as shown in Fig. 3(a). Also, the velocity field

$$v(\theta) := \omega + \kappa \int \sin(\theta' - \theta) p(\theta') d\theta' \quad (17)$$

is qualitatively different from that for the desynchronized state; the transition involves the emergence of the zeros of $v(\theta)$, and they continue to exist when κ or α is further increased. See the blue dashed and green dot-dashed curve in Fig. 3 for $v(\theta)$ just after and far beyond the transition, respectively. In contrast, $v(\theta)$ has no zero in the desynchronized state(the black solid curve in Fig. 3).

In deterministic systems, the zeros of the velocity field of the oscillators correspond to oscillation quenching, the phenomenon where the individual oscillators cease their oscillation[18]. Although our system involves stochastic

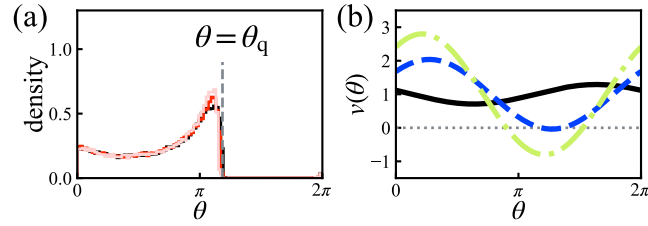


FIG. 3: SOQ occurs for sufficiently large κ . (a) Snapshots of the histogram of the phases in the system near the transition point of SOQ. The line colors are the same as that of FIG. 1(b,c). The parameters are $(\kappa, \alpha, \sigma) = (2.5, 0.5, 0.99)$. (b) The SOQ transition involves the emergens of the zeros of velocity field $v(\theta)$. The blue dotted and green dot-dashed curves show $v(\theta)$ for $\kappa = 2.2$, around which the SOQ transition occurs, and for $\kappa = 3.0$, where the system is far above the transition point, respectively. The black solid curve is for $\kappa = 0.3$, corresponding to the desynchronized state.

resetting, we can make an analogy as follows. Consider a “test oscillator,” i.e., an oscillator that changes its phase according to $v(\theta)$ but does not affect the system nor experience the resetting of its phase. If we put it into the system, its phase changes toward θ_q , a point at which $v(\theta) = 0$ and $dv(\theta)/d\theta \leq 0$ hold, and then becomes almost at rest after initial transients. Thus the steady distribution with which $v(\theta)$ has zeros implies the quenching of a test oscillator, and we refer to the realization of such a distribution as stochastic oscillation quenching (SOQ).

In the limit of $f(\theta) \rightarrow \delta(\theta)$, we can find the condition where $v(\theta)$ touches the line $v = 0$, or equivalently, $\frac{dv}{d\theta}(\theta_q) = 0$. To this end, we use a self-consistency argument as follows. Setting $\frac{\partial p}{\partial t} = 0$ in Eq. (7) and imposing $v(\theta_q) = \frac{dv}{d\theta}(\theta_q) = 0$, we obtain

$$[\cos(\theta_q - \theta) - 1] \frac{dp}{d\theta} + [\sin(\theta_q - \theta) - \alpha] p(\theta) + \alpha \delta(\theta) = 0. \quad (18)$$

We seek a solution $p(\theta)$ such that $p(\theta) > 0$ in $[0, \theta_q)$ and $p(\theta) = 0$ in $[\theta_q, 2\pi)$ because the phase of a new oscillator continues to approach from 0 to θ_q when SOQ occurs; see the distribution in FIG. 3(a), where $\sigma = 0.99 \simeq 1$. Noting that the derivative at a discontinuous point yields Dirac’s Delta function, we find such a solution as follows:

$$p(\theta) = \begin{cases} \frac{\alpha \exp \left[\alpha \left(\frac{1}{\tan \frac{\theta_q}{2}} - \frac{1}{\tan \frac{\theta_q - \theta}{2}} \right) \right]}{1 - \cos(\theta_q - \theta)} & (0 \leq \theta < \theta_q), \\ 0 & (\text{otherwise}), \end{cases} \quad (19)$$

which is continuous at $\theta = \theta_q$ but is discontinuous at $\theta = 0$.

Inserting Eq. (19) into Eq. (17) and imposing $v(\theta_q) = \frac{dv}{d\theta}(\theta_q) = 0$, we find that the parameters κ and α satisfy

$$\kappa = g_1(c_q(\alpha); \alpha) =: \kappa_q(\alpha), \quad (20)$$

where

$$g_1(c; \alpha) := \left(2\alpha e^{\frac{\alpha c}{\sqrt{1-c^2}}} \int_c^1 \frac{x e^{\frac{-\alpha x}{\sqrt{1-x^2}}}}{1-x^2} dx \right)^{-1}, \quad (21)$$

and $c_q := \cos \frac{\theta_q}{2}$ is a zero of the function

$$g_2(c; \alpha) = \int_c^1 \frac{(2x^2 - 1) e^{\frac{-\alpha x}{\sqrt{1-x^2}}}}{(1-x^2)^{3/2}} dx. \quad (22)$$

We solve $g_2 = 0$ numerically and insert the solutions into Eq. (20) to obtain κ_q , which is plotted as a solid yellow curve in FIG. 2(b). The curve agrees with the value of α above which Q vanishes for large κ , supporting that the disappearance of the collective oscillation is due to SOQ.

Conclusion We have analyzed a model of coupled oscillators with turnover and shown that the collective oscillation disappears via two types of transitions, namely, desynchronization and SOQ, depending on both the coupling strength and turnover rate. Importantly, SOQ occurs for sufficiently large coupling strength and is promoted not only by increasing the turnover rate but also by increasing the coupling strength. Thus this transition occurs not due to the turnover alone but due to the synergistic effect of the turnover and the interaction between oscillators. While it has already been reported that turnover may eliminate collective oscillation[13], understanding how this elimination occurs is essential for two reasons. Firstly, it helps us to avoid the unexpected disappearance of synchronized oscillations. Because increasing the coupling strength enhances the cohesiveness of the phases and promotes collective oscillation in the original Kuramoto model, one might expect the same would be true for oscillatory assemblies with turnover. However, increasing coupling strength may extinguish the collective oscillation through SOQ if the turnover rate is sufficiently large. Secondly, the type of transition may be exploited for designing appropriate forcing to steer the system to a desirable state, as has been done in Ref. [28]. Hence our results have potential implications for controlling and designing the collective behavior of oscillatory assemblies.

Previous experimental studies have proposed various open reactors that sustain non-equilibrium chemical reactions by controlling the flux into and out of the system[12, 29–31]. Desynchronization and SOQ may be observed if self-sustained oscillators are put into such an apparatus and parameters are varied. A candidate system might be constructed by combining techniques to maintain constant protein turnover[31] with protein molecules whose states change periodically[32, 33]. Our work might also be relevant to tissue formation in multicellular organisms because proliferation and differentiation sometimes involve phase resetting of cellular oscillators[34, 35].

Lastly, our model can easily be extended in many ways. A natural extension is to replace the Kuramoto model with other phase oscillator models. For example, our analyses can be straightforwardly extended to the case of the Kuramoto-Sakaguchi model, which will be reported elsewhere[36].

* corresponding author: aozawa@g.ecc.u-tokyo.ac.jp

- [1] A Pikovsky, M Rosenblum, and J Kurths. *Synchronization: A Universal Concept in Nonlinear Sciences*. Cambridge University Press, Cambridge, 2001.
- [2] Leon Glass. Synchronization and rhythmic processes in physiology. *Nature*, Vol. 410, No. 6825, pp. 277–284, 2001.
- [3] A T Winfree. *The Geometry of Biological Time*. Springer New York, New York, 2001.
- [4] Steven H Strogatz, Daniel M Abrams, Allan McRobie, Bruno Eckhardt, and Edward Ott. Crowd synchrony on the Millennium Bridge. *Nature*, Vol. 438, No. 7064, pp. 43–44, 2005.
- [5] Z Néda, E Ravasz, Y Brechet, T Vicsek, and A.-L. Barabási. The sound of many hands clapping. *Nature*, Vol. 403, No. 6772, pp. 849–850, 2000.
- [6] Miguel C. Soriano, Jordi García-Ojalvo, Claudio R. Mirasso, and Ingo Fischer. Complex photonics: Dynamics and applications of delay-coupled semiconductor lasers. *Reviews of Modern Physics*, Vol. 85, No. 1, pp. 421–470, March 2013.
- [7] Kurt Wiesenfeld, Pere Colet, and Steven H. Strogatz. Synchronization Transitions in a Disordered Josephson Series Array. *Physical Review Letters*, Vol. 76, No. 3, pp. 404–407, January 1996.
- [8] Zach Rolfs, Brian L Frey, Xudong Shi, Yoshitaka Kawai, Lloyd M Smith, and Nathan V Welham. An atlas of protein turnover rates in mouse tissues. *Nature Communications*, Vol. 12, No. 1, p. 6778, 2021.
- [9] Jason Pellettier and Alejandro Sánchez Alvarado. Cell Turnover and Adult Tissue Homeostasis: From Humans to Planarians. *Annual Review of Genetics*, Vol. 41, No. 1, pp. 83–105, December 2007.
- [10] Chris Burnett, Timothy Norman, and Katia Sycara. Trust Decision-Making in Multi-Agent Systems. In *Proceedings of the 22nd International Joint Conference on Artificial Intelligence*, p. 120, Barcelona, Catalonia, Spain, January 2011.
- [11] Stanislao Gualdi, Jean-Philippe Bouchaud, Giulia Cencetti, Marco Tarzia, and Francesco Zamponi. Endogenous Crisis Waves: Stochastic Model with Synchronized Collective Behavior. *Physical Review Letters*, Vol. 114, No. 8, p. 088701, February 2015.
- [12] Haruka Sugiura, Manami Ito, Tomoya Okuaki, Yoshihito Mori, Hiroyuki Kitahata, and Masahiro Takinoue. Pulse-density modulation control of chemical oscillation far from equilibrium in a droplet open-reactor system. *Nature Communications*, Vol. 7, No. 1, p. 10212, 2016.
- [13] David Zwicker, David K Lubensky, and Pieter Rein ten Wolde. Robust circadian clocks from coupled protein-modification and transcription–translation cycles. *Proceedings of the National Academy of Sciences*, Vol. 107, No. 52, pp. 22540–22545, December 2010.
- [14] Wen Yu and Kevin B. Wood. Synchronization and phase redistribution in self-replicating populations of coupled oscillators and excitable elements. Vol. 91, No. 6, p. 062708, June 2015.
- [15] Keiko Imai, Taeko Nishiwaki, Takao Kondo, and Hideo Iwasaki. Circadian Rhythms in the Synthesis and Degradation of a Master Clock Protein KaiC in Cyanobacteria *. *Journal of Biological Chemistry*, Vol. 279, No. 35, pp. 36534–36539, August 2004.
- [16] Shu-Wen Teng, Shankar Mukherji, Jeffrey R Moffitt, Sophie de Buyl, and Erin K O’Shea. Robust Circadian Oscillations

- in Growing Cyanobacteria Require Transcriptional Feedback. *Science*, Vol. 340, No. 6133, pp. 737–740, 2013.
- [17] Y Kuramoto. *Chemical Oscillations, Waves, and Turbulence*. Springer, Berlin, 1984.
- [18] Wei Zou, D V Senthilkumar, Meng Zhan, and Jürgen Kurths. Quenching, aging, and reviving in coupled dynamical networks. *Physics Reports*, Vol. 931, pp. 1–72, 2021.
- [19] Yoshiki Kuramoto. Self-entrainment of a population of coupled non-linear oscillators. *Lect. Notes Phys.*, Vol. 39, pp. 420–422, 1975.
- [20] Steven H Strogatz. From Kuramoto to Crawford: Exploring the onset of synchronization in populations of coupled oscillators. *Physica D: Nonlinear Phenomena*, Vol. 143, No. 1, pp. 1–20, 2000.
- [21] Juan A. Acebrón, L. L. Bonilla, Conrad J. Pérez Vicente, Félix Ritort, and Renato Spigler. The Kuramoto model: A simple paradigm for synchronization phenomena. *Reviews of Modern Physics*, Vol. 77, No. 1, pp. 137–185, April 2005.
- [22] Yumei Zhai, István Z Kiss, Hiroaki Daido, and John L Hudson. Extracting order parameters from global measurements with application to coupled electrochemical oscillators. *Physica D: Nonlinear Phenomena*, Vol. 199, No. 3, pp. 387–399, 2004.
- [23] István Z Kiss, Yumei Zhai, and John L Hudson. Emerging Coherence in a Population of Chemical Oscillators. *Science*, Vol. 296, No. 5573, pp. 1676–1678, May 2002.
- [24] Martin R Evans, Satya N Majumdar, and Grégory Schehr. Stochastic resetting and applications. *Journal of Physics A: Mathematical and Theoretical*, Vol. 53, No. 19, p. 193001, 2020.
- [25] Floyd B. Hanson. *Applied Stochastic Processes and Control for Jump-diffusions : Modeling, Analysis, and Computation*. Society for Industrial and Applied Mathematics, Philadelphia, 2007.
- [26] John D. Crawford and K. T. R. Davies. Synchronization of globally coupled phase oscillators: Singularities and scaling for general couplings. *Physica D: Nonlinear Phenomena*, Vol. 125, No. 1, pp. 1–46, January 1999.
- [27] Jun Sakurai and Jim Napolitano. *Modern Quantum Mechanics*. Addison-Wesley, Boston, 2nd ed edition, 2011.
- [28] Yoriko Murayama, Hiroshi Kori, Chiaki Oshima, Takao Kondo, Hideo Iwasaki, and Hiroshi Ito. Low temperature nullifies the circadian clock in cyanobacteria through Hopf bifurcation. *Proceedings of the National Academy of Sciences*, Vol. 114, No. 22, pp. 5641–5646, May 2017.
- [29] Irving R. Epstein. The role of flow systems in far-from-equilibrium dynamics. *Journal of Chemical Education*, Vol. 66, No. 3, p. 191, March 1989.
- [30] Alexander S. Spirin. High-throughput cell-free systems for synthesis of functionally active proteins. *Trends in Biotechnology*, Vol. 22, No. 10, pp. 538–545, October 2004.
- [31] Henrike Niederholtmeyer, Viktoria Stepanova, and Sebastian J. Maerkl. Implementation of cell-free biological networks at steady state. *Proceedings of the National Academy of Sciences*, Vol. 110, No. 40, pp. 15985–15990, October 2013.
- [32] Ofer Kimchi, Carl P. Goodrich, Alexis Courbet, Agnese I. Curatolo, Nicholas B. Woodall, David Baker, and Michael P. Brenner. Self-assembly-based posttranslational protein oscillators. *Science Advances*, Vol. 6, No. 51, p. eabc1939, December 2020.
- [33] Masato Nakajima, Keiko Imai, Hiroshi Ito, Taeko Nishiwaki, Yoriko Murayama, Hideo Iwasaki, Tokitaka Oyama, and Takao Kondo. Reconstitution of Circadian Oscillation of Cyanobacterial KaiC Phosphorylation in Vitro. *Science*, Vol. 308, No. 5720, pp. 414 LP – 415, April 2005.
- [34] Hirokazu Fukuda, Kazuya Ukai, and Tokitaka Oyama. Self-arrangement of cellular circadian rhythms through phase-resetting in plant roots. *Physical Review E*, Vol. 86, No. 4, p. 041917, October 2012.
- [35] Kazuhiro Yagita, Kyoji Horie, Satoshi Koinuma, Wataru Nakamura, Iori Yamanaka, Akihiro Urasaki, Yasufumi Shigeyoshi, Koichi Kawakami, Shoichi Shimada, Junji Takeda, and Yasuo Uchiyama. Development of the circadian oscillator during differentiation of mouse embryonic stem cells in vitro. *Proceedings of the National Academy of Sciences*, Vol. 107, No. 8, pp. 3846–3851, February 2010.
- [36] Ayumi Ozawa and Hiroshi Kori. in preparation.